

BEHAVIOR OF A BUBBLE IN DIELECTRIC LIQUID IN UNIFORM AND NON-UNIFORM ELECTRIC FIELDS

A.A. Nemykina^{1,2} & D.A. Medvedev^{1,2,*}

¹Lavrentyev Institute of Hydrodynamics SB RAS, Novosibirsk, Russia

²Novosibirsk State University, Novosibirsk, Russia

*Address all correspondence to: D.A. Medvedev, Lavrentyev Institute of Hydrodynamics SB RAS, Novosibirsk, Russia, E-mail: dmedv@hydro.nsc.ru

Original Manuscript Submitted: 10/1/2019; Final Draft Received: 12/29/2019

We simulated the behavior of vapor and gas–vapor bubbles in dielectric liquid under the action of an electric field. The thermal multiphase lattice Boltzmann method was used to calculate the fluid dynamics. After applying the electric voltage, the bubble was deformed. In the uniform field (in which electrodes occupied all of the boundaries), the bubble was elongated along the direction of the average electric field and the degree of deformation was then calculated, which was close to experimentally obtained results. When the electrodes were smaller than the size of the computational domain, the field was non-uniform. The field magnitude was higher between the electrodes and decreased outside of the electrodes. In this case, the bubble was stretched in the direction normal to the electric field due to the forces acting on the inhomogeneous dielectric fluid. Moreover, for sufficiently small electrodes, the bubble escaped outside of the electrodes. This type of interesting behavior has been previously observed in experiments of Korobeynikov et al.

KEY WORDS: electrohydrodynamics, bubbles, bubble deformation, lattice Boltzmann method

1. INTRODUCTION

Two-phase fluid systems (droplets, foams, and bubbles in liquid) with phase transitions between the liquid and vapor are widely used in science and engineering. For example, they are applied in cooling devices. Electric fields are often used to control the fluid systems. Among the applications, one can list electrohydrodynamic pumps, electrowetting, jet printing, etc.

Understanding the behavior of bubbles in dielectric liquids under the action of an electric field is an important scientific and practical problem. Such bubbles are present or generated in liquid insulation of power electrical equipment where they can serve as one of the most frequent sources of the inception of electric breakdown (Krasucki, 1966; Tsujikawa et al., 1988; Talaat and El-Zein, 2012). Besides this, bubbles under the action of an electric field play an important role in different technical processes. Many experimental and theoretical works are devoted to the investigation of such bubbles (Garton and Krasucki, 1964; Krasucki, 1966; Ogata et al., 1985; Beroual, 1992; Kupershtokh and Medvedev, 2006; Liu et al., 2008; Shaw and Spelt, 2009; Talaat and El-Zein, 2012; Borthakur et al., 2018). The equilibrium shape of a bubble placed at the wall was investigated numerically by Wang et al. (2017a), and the behavior of a bubble rising in parallel gravitational and electric fields was simulated in Wang et al. (2017b). The shape of a conductive bubble in an electric field was investigated theoretically in Zubarev and Zubareva (2015). The experimental investigation of the influence of an electric field on bubbles during boiling was carried out in Masoudnia and Fatahi (2016).

However, numerical simulations of the non-stationary behavior of bubbles in an electric field are rare. This is mainly due to the complexity of computer simulations of two-phase gas–liquid systems that take into account surface tension and electrical forces. Recently, a new method of computer modeling of such processes has appeared. The method of lattice Boltzmann equations (McNamara and Zanetti, 1988; Qian et al., 1992; Koelman, 1991; Kupershtokh and Medvedev, 2006) is a powerful tool for modeling such complex multiphysical phenomena.

NOMENCLATURE

A	free parameter in the forcing scheme	Greek Symbols	
a	large axis of ellipsoid	α	polarizability in the Clausius–Mossotti formula
b	small axis of ellipsoid	Δ	deformation of a bubble
\mathbf{c}_k	velocity of pseudoparticles	ε	electric permittivity
C_V	specific heat at constant volume	ε_0	electrostatic constant
Ca	electrical capillary number	θ	kinetic temperature
E	electric field	ν	kinetic viscosity
\mathbf{F}	force acting on a fluid	ρ	fluid density
g_k	energy distribution function	σ	surface tension
\dot{N}_k	distribution function for the lattice Boltzmann method	τ	non-dimensional relaxation time
N_k^{eq}	equilibrium distribution function	Φ	special function in the forcing scheme
P	fluid pressure	φ	electric potential
R_0	initial radius of a bubble	Ω	collision operator
T	fluid temperature		
\mathbf{u}	fluid velocity	Subscripts	
U	pseudopotential	c	critical value
W	density of internal energy	L	liquid
w_k	weight in the lattice Boltzmann equation	V	vapor

This work is devoted to the numerical simulation of a bubble in a dielectric liquid placed between two flat electrodes with a DC electric voltage applied to them. Then, the time evolution of the bubble is simulated by the lattice Boltzmann method.

2. NUMERICAL METHOD

2.1 Lattice Boltzmann Method for Multiphase Fluid Dynamics

We use the lattice Boltzmann method to simulate the dynamics of multiphase fluids. This method considers the fluid as an ensemble of pseudoparticles moving along the links of a regular spatial lattice. The velocities of the pseudoparticles take a limited set of values such that the particle propagates in a neighbor lattice node during one time step. One-particle distribution functions (N_k) are the main variables, the evolution of which is governed by the following equation:

$$N_k(\mathbf{x} + \mathbf{c}_k \Delta t, t + \Delta t) = N_k(\mathbf{x}, t) + \Omega_k(N_k) + \Delta N_k \quad (1)$$

The discrete velocities values $|c_k| = 0, h/\Delta t$ and $\sqrt{2}h/\Delta t$ for the two-dimensional model D2Q9 and the three-dimensional model D3Q19 were used in this work. Here, h is the lattice spacing and Δt is the time step.

The collision operator Ω_k is taken in the following Bhatnagar–Gross–Krook form (Qian et al., 1992)

$$\Omega_k[N_k(\mathbf{x}, t)] = \frac{N_k^{\text{eq}}(\rho, \mathbf{u}) - N_k(\mathbf{x}, t)}{\tau}$$

which is the relaxation to a local equilibrium. The dimensionless relaxation time τ determines the kinematic viscosity of the fluid: $\nu = (\tau - 1/2)\theta \Delta t$. The equilibrium relaxation functions are usually taken in the form of truncated Maxwellian distributions (Koelman, 1991)

$$N_k^{\text{eq}}(\rho, \mathbf{u}) = \rho w_k \left(1 + \frac{(\mathbf{c}_k \cdot \mathbf{u})}{\theta} + \frac{(\mathbf{c}_k \cdot \mathbf{u})^2}{2\theta^2} - \frac{\mathbf{u}^2}{2\theta} \right) \quad (2)$$

The kinetic temperature is $\theta = (h/\Delta t)^2$. The hydrodynamic values are calculated as the zeroth and first moments of N_k

$$\rho = \sum_k N_k, \quad \rho \mathbf{u} = \sum_k N_k \mathbf{c}_k$$

The change in distribution functions (ΔN_k) due to the action of volume forces is calculated using the exact difference method (Kupershtokh, 2010)

$$\Delta N_k = N_k^{\text{eq}}(\rho, \mathbf{u} + \Delta \mathbf{u}) - N_k^{\text{eq}}(\rho, \mathbf{u})$$

The liquid–vapor phase transitions are simulated by introducing the internal forces between nodes as the gradient of the pseudopotential $\mathbf{F}_{int}(\mathbf{x}) = -\nabla U$, where the pseudopotential is defined by the equation of state for the fluid: $U = P(\rho, T) - \rho\theta$ (Qian and Chen, 1997). A special function, $\Phi = \sqrt{-U}$, was introduced in Kupershtokh et al. (2007, 2009), and the formula for the internal forces was rewritten in the equivalent form

$$\mathbf{F}(\mathbf{x}) = 2A\nabla(\Phi^2) + (1 - 2A)2\Phi\nabla\Phi$$

Here, A is a free parameter that allows one to tune the coexistence curve in accordance with the equation of state. The wetting of the rigid boundaries is simulated by setting the constant value of Φ in the boundary nodes.

We use the reduced variables $\tilde{T} = T/T_c$, $\tilde{P} = P/P_c$, and $\tilde{\rho} = \rho/\rho_c$, where T_c , P_c , and ρ_c are the values of the temperature, pressure, and density, respectively, at the critical point. The Van der Waals equation of state is used for the fluid, which takes the following form:

$$\tilde{P} = \frac{8\tilde{\rho}\tilde{T}}{3 - \tilde{\rho}} - 3\tilde{\rho}^2 \quad (3)$$

2.2 Heat Transport Simulation

The advection of heat is described by the introduction of a second set of distribution functions representing the density of internal energy

$$W = C_V \rho T = \sum g_k$$

Here, C_V is the specific heat at constant volume. The evolution equation for these distribution functions is similar to Eq. (1):

$$g_k(\mathbf{x} + \mathbf{c}_k \Delta t, t + \Delta t) = g_k(\mathbf{x}, t) + \frac{g_k^{\text{eq}} - g_k}{\tau_E} + \Delta g_k$$

The equilibrium distribution functions are taken in the form of Eq. (2), where \mathbf{u} is the velocity of the fluid. The change in the distribution functions (Δg_k) consists of two parts. The first one includes all of the sources: the pressure work and the release or absorption of the latent heat of phase transitions. When the change in the internal energy density due to the sources is equal to ΔW , the corresponding changes of the distribution functions are calculated by

$$\Delta g_k^{(1)} = g_k \Delta W / W$$

Special pseudoforces are introduced in order to prevent the non-physical energy from spreading at the phase boundaries. They result in a change in the distribution functions expressed as

$$\Delta g_k^{(2)} = g_k^{\text{eq}}(W, \mathbf{u} + \Delta \mathbf{u}) - g_k^{\text{eq}}(W, \mathbf{u})$$

Here, $\Delta \mathbf{u} = \mathbf{F}\Delta t/\rho$ is the change of the fluid velocity at a node under the action of forces (interaction forces providing the phase transition, electric forces, gravity forces, and so on). For a more detailed description of the method, see Kupershtokh et al. (2018). The heat conduction is calculated using the explicit finite-difference numerical scheme.

2.3 Electric Potential and Electric Force Calculations

The Poisson's equation for electric potential ϕ in the fluid with variable electric permittivity

$$\nabla \cdot (\varepsilon \nabla \phi) = 0$$

is solved at each time step using simple iterations. The iterations are repeated until the relative change in the electric potential becomes smaller than a certain value, $|\Delta\phi/\phi| < 10^{-8}$. The distribution of the electric field strength is then calculated by the equation $\mathbf{E} = -\nabla\phi$.

The density dependence of the electric permittivity is described with the Clausius–Mossotti formula

$$\varepsilon = 1 + \frac{3\alpha\rho}{1 - \alpha\rho}$$

The coefficient α (polarizability) is defined by setting the value of permittivity for the liquid phase: $\varepsilon_L = \varepsilon(\rho_L)$. The force acting on an inhomogeneous fluid in the electric field is calculated using the Helmholtz formula (Landau and Lifshitz, 1959)

$$\mathbf{F} = -\frac{\varepsilon_0 E^2}{2} \nabla \varepsilon + \frac{\varepsilon_0}{2} \nabla \left[E^2 \rho \left(\frac{\partial \varepsilon}{\partial \rho} \right)_T \right]$$

The calculations were performed in a rectangular area with rigid electrodes at the top and bottom boundaries [with fixed values of the electric potential at the bottom ($\phi = 0$) and top ($\phi = V$)] and periodic side boundaries.

3. RESULTS

3.1 Bubbles in a Uniform Field

The fluid with the Van der Waals equation of state [Eq. (3)] was simulated. The initial reduced temperature was $\tilde{T} = 0.7$. The size of the calculation region was $200 \times 200 \times 320$ grid points. The relative influence of the electric field was characterized by the electrical capillary number $Ca = \varepsilon_0 (\varepsilon - 1) E^2 R_0 / (4\pi\sigma)$ (the electrical Bond number), where σ is the surface tension. The permittivity of the liquid phase was $\varepsilon_L = 2.2$. We simulated the dynamics of a bubble for $Ca = 20, 40,$ and 80 (where the capillary number was changed by the change in the electric field magnitude). Figure 1 shows the process of bubble deformation for $Ca = 80$ (where the fluid density in a central plane is shown). This capillary number corresponds to a bubble radius of 1 mm, surface tension of $\sigma = 0.05$ N/m, and an average electric field magnitude of $E_0 = 5.5 \times 10^6$ V/m (55 kV/cm). After applying the voltage, the bubble begins to elongate along the direction of the electric field, and the value of elongation increases with the increasing electric field.

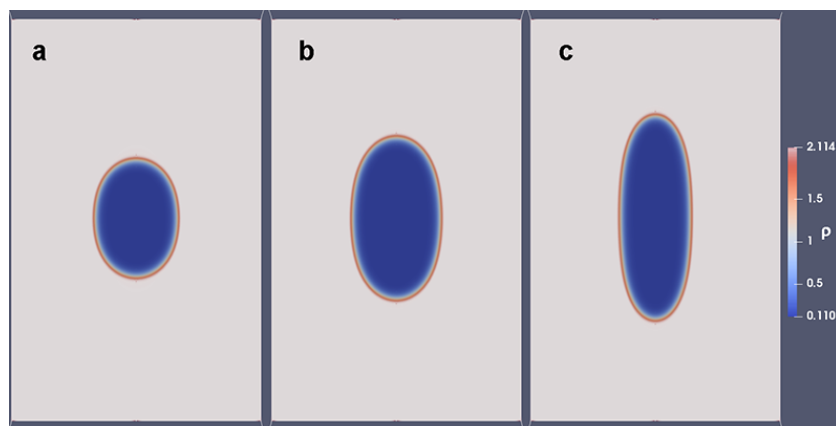


FIG. 1: Deformation of a bubble in an electric field (time in lattice units): (a) $t = 500$; (b) $t = 1000$; (c) $t = 3000$

The deformation of the bubble can be described quantitatively by the value $\Delta = (a - b)/b$, where a and b are the large and the small axes of an ellipsoid, respectively. The time evolution of the bubble deformation for different capillary numbers is shown in Fig. 2. The value of the deformation for $Ca = 20$ is $\Delta = 0.36$. In experiments with transformer oil (Korobeynikov et al., 2019), the observed deformation was 0.46 for the somewhat larger capillary number of $Ca = 29$. Theoretical calculations in linear approximation (Korobeynikov, 1979) provide the value of $\Delta = 0.28$, which is smaller than the value obtained in our calculations. The reason of this discrepancy can be the moderate size of the calculation region due to the computational restrictions. Thus, we observed reasonable agreement with the experimental and theoretical results, keeping in mind some difference in the problem setup. For large capillary numbers ($Ca = 80$), the oscillations of the bubble shape are visible on the graph. These oscillations are caused by the hydrodynamic flows produced due to the deformation of the bubble.

3.2 Bubbles in a Non-Uniform Field

We investigated the dynamics of a bubble in an electric field for different sizes of electrodes. In the case of infinite electrodes (a nearly uniform electric field), the bubble elongates along the field and can even break up into two smaller bubbles (for large field values). However, in reality, electrodes are not infinite, thus the influence of edge effects could be crucial. In the simulations, we used a rectangular region with 1536×512 grid units, and the initial radius of the bubble was about 60 grid units. The Van der Waals equation of state [Eq. (3)] was used with the reduced temperature $\tilde{T} = 0.8$. The electric permittivity of the liquid phase was $\epsilon_L = 2$ and the average field magnitude was $\langle E \rangle = 0.15$, which corresponds to capillary number $Ca = 37$.

In the first calculation, the length of the electrodes was 512 grid units, which was much larger than the bubble size. The distribution of the electric field for this case is shown in Fig. 3. The bubble stretched along the field (directed vertically) and then reached its new equilibrium state (Fig. 4). When the length of the electrodes was 192 grid units, which was comparable to the bubble size, the degree of the field non-uniformity was high (Fig. 5) and the bubble stretched across the field. The position between the electrodes was unstable, thus the bubble moved to the area with the lower field value (Fig. 6). The bubble was able to deviate to the left or right, which depended on the initial position of the center of the bubble relative to the computational grid. Even in an ideal symmetrical position, the balance was unstable and broke. When the bubble escaped from the region between the electrodes, the force due to the non-uniform field no longer stretched the bubble but pushed it sideways [Figs. 6(e) and 6(f)]. However, the stretching along the field lines remained and the bubble was stretched vertically [Fig. 6(f)].

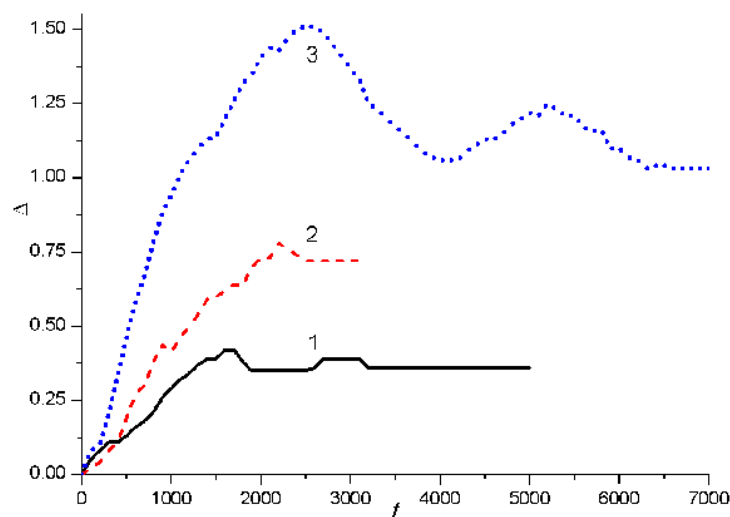


FIG. 2: Deformation of a bubble in an electric field (time in lattice units): $Ca = 20$ (curve 1); $Ca = 40$ (curve 2); $Ca = 80$ (curve 3)

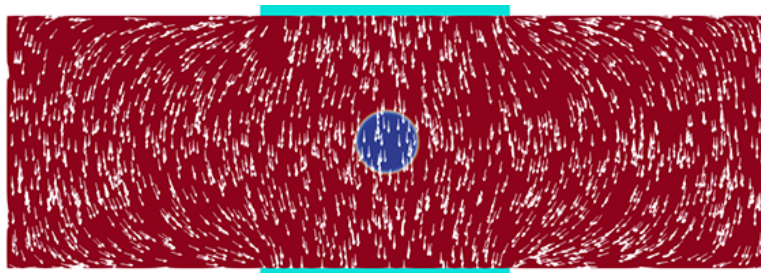


FIG. 3: The electric field for the electrode length of 512 grid units

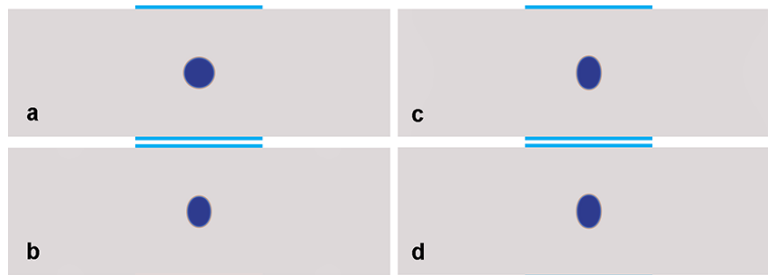


FIG. 4: Dynamics of a bubble for the electrode length of 512 grid units (time in lattice units): (a) $t = 10,000$; (b) $t = 15,000$; (c) $t = 30,000$; (d) $t = 45,000$

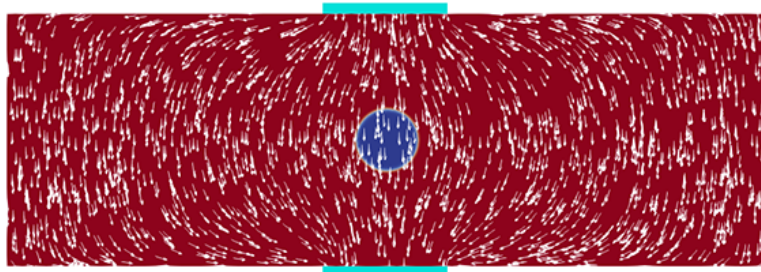


FIG. 5: Electric field for the electrode length of 192 grid units

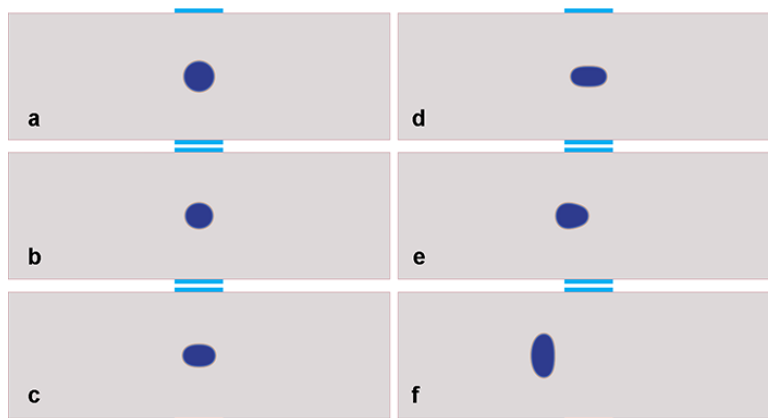


FIG. 6: Dynamics of a bubble for the electrode length of 192 grid units (time in lattice units): (a) $t = 10,000$; (b) $t = 15,000$; (c) $t = 30,000$; (d) $t = 50,000$; (e) $t = 70,000$; (f) $t = 80,000$

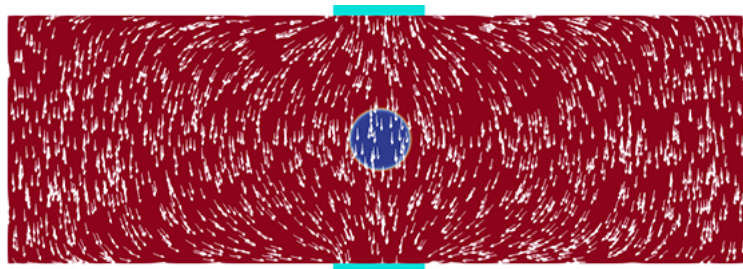


FIG. 7: Electric field for the electrode length of 256 grid units

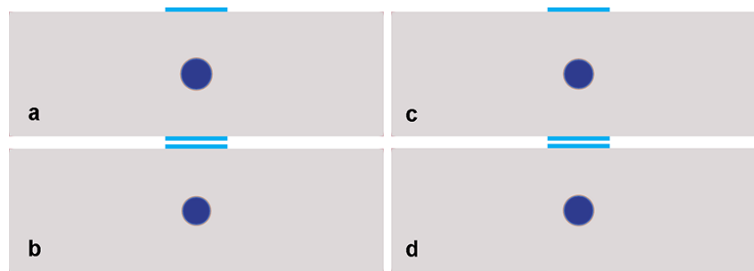


FIG. 8: Dynamics of a bubble for the electrode length of 256 grid units (time in lattice units): (a) $t = 10,000$; (b) $t = 15,000$; (c) $t = 30,000$; (d) $t = 45,000$

When the length of the electrodes was 256 grid units, the degree of non-uniformity of the electric field was intermediate between the two previous cases (Fig. 7). In this case, the effects of stretching along the field and the perpendicular pulling were close. Under the action of the non-uniform electric field, the bubble stretched, expanded somewhat (Fig. 8), and finally acquired its equilibrium state, which was almost round in this intermediate regime.

4. CONCLUSIONS

We investigated numerically the behavior of bubbles in a dielectric liquid under the action of an electric field. In a uniform field, the bubble elongated along the field lines, and the degree of elongation increased with the increasing magnitude of the field. The deformation of a bubble in the calculations agreed with the experimental results. In a non-uniform electric field, the bubble also stretched in the direction across the field. For a moderately non-uniform field, the bubble retained a round shape. When the non-uniformity of the field was high (for sufficiently small electrodes), the elongation across the field prevailed. In this case, the bubble position between electrodes was unstable, and the bubble escaped into the region of the lower field.

ACKNOWLEDGMENT

This work was partially supported by the Russian Science Foundation (Project No. 16-19-10229).

REFERENCES

- Beroual, A., Behaviour of Charged and Uncharged Bubbles in Dielectric Liquids Subjected to Electric Stress, *J. Appl. Phys.*, vol. **71**, no. 3, pp. 1142–1145, 1992.
- Borthakur, M.P., Biswas, G., and Bandyopadhyay, D., Dynamics of Drop Formation from Submerged Orifices under the Influence of Electric Field, *Phys. Fluids*, vol. **30**, p. 122104, 2018.
- Garton, C.G. and Krasucki, Z., Bubbles in Insulating Liquids: Stability in an Electric Field, *Proc. R. Soc.*, vol. **A280**, no. 1381, pp. 211–226, 1964.

- Koelman, J.M.V.A., A Simple Lattice Boltzmann Scheme for Navier–Stokes Fluid Flow, *Europhys. Lett.*, vol. **15**, no. 6, pp. 603–607, 1991.
- Korobeynikov, S.M., Bubble Deformation in an Electric Field, *J. Eng. Phys.*, vol. **36**, no. 5, pp. 588–589, 1979.
- Korobeynikov, S.M., Ridel, A.V., and Medvedev, D.A., Deformation of Bubble in Transformer Oil at the Action of Alternating Electric Field, *Eur. J. Mech. B Fluids*, vol. **75**, pp. 105–109, 2019.
- Krasucki, Z., Breakdown of Liquid Dielectrics, *Proc. R. Soc.*, vol. **A294**, no. 1438, pp. 393–404, 1966.
- Kupershtokh, A.L., Criterion of Numerical Instability of Liquid State in LBE Simulations, *Comput. Math. Appl.*, vol. **59**, no. 7, pp. 2236–2245, 2010.
- Kupershtokh, A.L., Karpov, D.I., Medvedev, D.A., Stamatelatos, C.P., Charalambakos, V.P., Pyrgioti, E.C., and Agoris, D.P., Stochastic Models of Partial Discharge Activity in Solid and Liquid Dielectrics, *IET Sci. Meas. Technol.*, vol. **1**, no. 6, pp. 303–311, 2007.
- Kupershtokh, A.L. and Medvedev, D.A., Lattice Boltzmann Method in Electrohydrodynamic Problems, *J. Electrostat.*, vol. **64**, nos. 7–9, pp. 581–585, 2006.
- Kupershtokh, A.L., Medvedev, D.A., and Gribanov, I.I., Thermal Lattice Boltzmann Method for Multiphase Flows, *Phys. Rev. E*, vol. **98**, no. 2, p. 023308, 2018.
- Kupershtokh, A.L., Medvedev, D.A., and Karpov, D.I., On Equations of State in a Lattice Boltzmann Method, *Comput. Math. Appl.*, vol. **58**, no. 5, pp. 965–974, 2009.
- Landau, L.D. and Lifshitz, E.M., *Electrodynamics of Continuous Media*, Oxford, U.K.: Pergamon Press, 1959.
- Liu, Y., Oh, K., Bai, J.G., Chang, C.-L., Yeo, W., Chung, J.-H., Lee, K.-H., and Liu, W.K., Manipulation of Nanoparticles and Biomolecules by Electric Field and Surface Tension, *Comput. Methods Appl. Mech. Eng.*, vol. **197**, nos. 25–28, pp. 2156–2172, 2008.
- Masoudnia, M. and Fatahi, M., Electric Field Effect on the Rise of Single Bubbles during Boiling, *Int. J. Mech. Mech. Eng.*, vol. **10**, no. 6, pp. 1138–1143, 2016.
- McNamara, G.R. and Zanetti, G., Use of the Boltzmann Equation to Simulate Lattice-Gas Automata, *Phys. Rev. Lett.*, vol. **61**, no. 20, pp. 2332–2335, 1988.
- Ogata, S., Tan, K., Nishijima, K., and Chang, J.-S., Development of Improved Bubble Disruption and Dispersion Technique by an Applied Electric Field Method, *AIChE J.*, vol. **31**, no. 1, pp. 62–69, 1985.
- Qian, Y.H. and Chen, S., Finite Size Effect in Lattice-BGK Models, *Int. J. Mod. Phys. C*, vol. **8**, no. 4, pp. 763–771, 1997.
- Qian, Y.H., d’Humières, D., and Lallemand, P., Lattice BGK Models for Navier–Stokes Equation, *Europhys. Lett.*, vol. **17**, no. 6, pp. 479–484, 1992.
- Shaw, S.J. and Spelt, P.D.M., Critical Strength of an Electric Field Whereby a Bubble Can Adopt a Steady Shape, *Proc. R. Soc. A*, vol. **465**, no. 2110, pp. 3127–3143, 2009.
- Talaat, M. and El-Zein, A., Analysis of Air Bubble Deformation Subjected to Uniform Electric Field in Liquid Dielectric, *Int. J. Electromagn. Appl.*, vol. **2**, no. 1, pp. 4–10, 2012.
- Tsujikawa, Y., Onoda, M., Nakayama, H., and Amakawa, K., Partial Discharge in a Void Filled with Sulfur Hexafluoride and Formation of Sulfide, *Jpn. J. Appl. Phys.*, vol. **27/2**, no. 3, pp. L451–L453, 1988.
- Wang, H., Liu, L., and Liu, D., Equilibrium Shapes of a Heterogeneous Bubble in an Electric Field: A Variational Formulation and Numerical Verification, *Proc. R. Soc. A*, vol. **473**, no. 2199, p. 20160744, 2017a.
- Wang, Y., Sun, D., Zhang, A., and Yu, B., Numerical Simulation of Bubble Dynamics in the Gravitational and Uniform Electric Field, *Numer. Heat Transf., Part A*, vol. **71**, no. 10, pp. 1034–1051, 2017b.
- Zubarev, N.M. and Zubareva, O.V., Exact Solutions for the Evolution of a Bubble in an Ideal Liquid in a Uniform External Electric Field, *J. Exp. Theor. Phys.*, vol. **120**, pp. 155–160, 2015.